Multiferroic IR vibrational modes in $LiNiPO_4$

S.A. Klimin[1], M.S. Radionov[1], A.Yu. Glamazda[2], A.V. Peschanskii[2]

[1]Institute of Spectroscopy, Russian Academy of Sciences, Moscow, 108840, Troitsk, Russia

[2]B. Verkin Institute for Low Temperature Physics and Engineering of the National Academy of Sciences of Ukraine, 47 Nauky Ave., 61103 Kharkov, Ukraine

The olivine-type lithium orthophosphates LiMPO$_4$ (M=Fe^{2+}, Mn^{2+}, Co^{2+}, Ni^{2+}) family has intriguing magnetoelectric properties and the entangled spin excitations. They demonstrate a tight coupling of the phonon, electron and magnetic subsystems.

The substantial interest in olivine-structured orthophosphate $LiNiPO_4$ is caused by its possible application as the electrode material in the batteries and as multiferroic element in magnetoelectric devices. The present work is aimed at examining more closely the lattice excitations in the $LiNiPO_4$ single crystal by the combination of the polarized IR reflectance spectroscopy in the temperature range of 7-300 K and lattice dynamic calculations.

At low temperatures, the measurements of infrared reflection (IR) spectra were carried out using BRUKER IFS125 Fourier spectrometer equiped with a helium bolometer (50-700 cm^{-1}) and MCT detector cooled with liquid nitrogen (700-5000 cm^{-1}). The sample was cooled in a CRYOMECH PT403 closed-cycled helium cryostat with polyethylene windows.

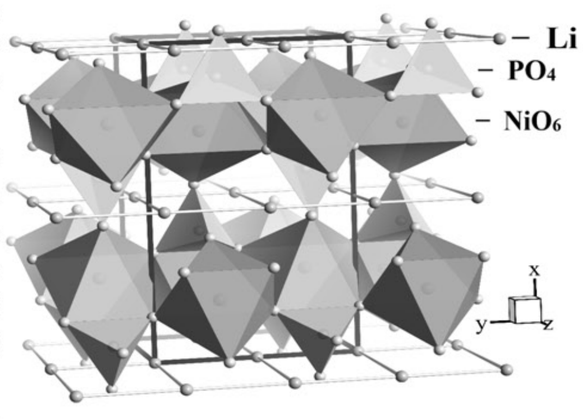

Fig. 1. Structure of $LiNiPO_4$.

$LiNiPO_4$: $Pnma$ (D_{2h}^{16}), Z=4,

a=10.032 A, b=5.854 A, c=4.677 A at T=300 K,

a=10.102 A, b=5.83 A, c=4.66 A at T < T_N.

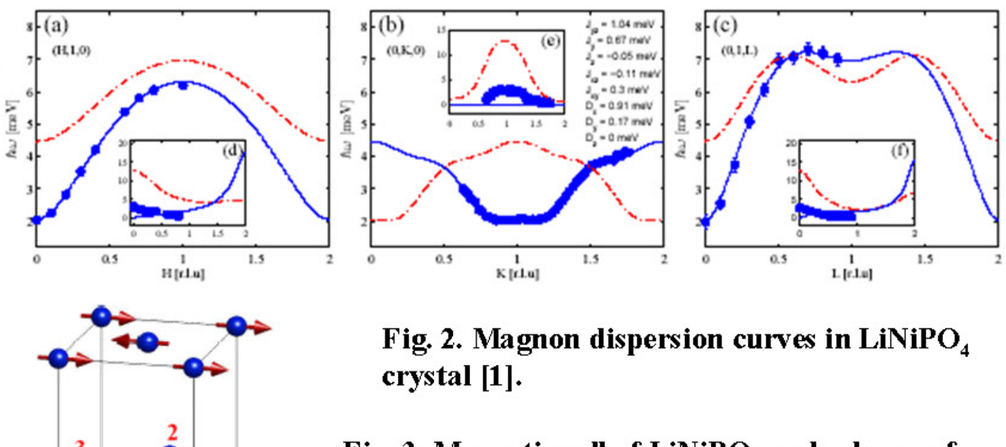

Fig. 2. Magnon dispersion curves in $LiNiPO_4$ crystal [1].

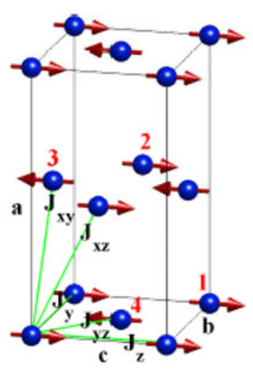

Fig. 3. Magnetic cell of $LiNiPO_4$ and scheme of exchange interactions. Ni^{2+} ions are showed [1]. Parameters of model (in meV):

J_{yz}	J_y	J_z	J_{xz}	J_{xy}	D_x	D_y	D_z
1.036	0.6701	−0.0469	−0.1121	0.2977	0.1696	0.9097	0

Previous IR data [2]

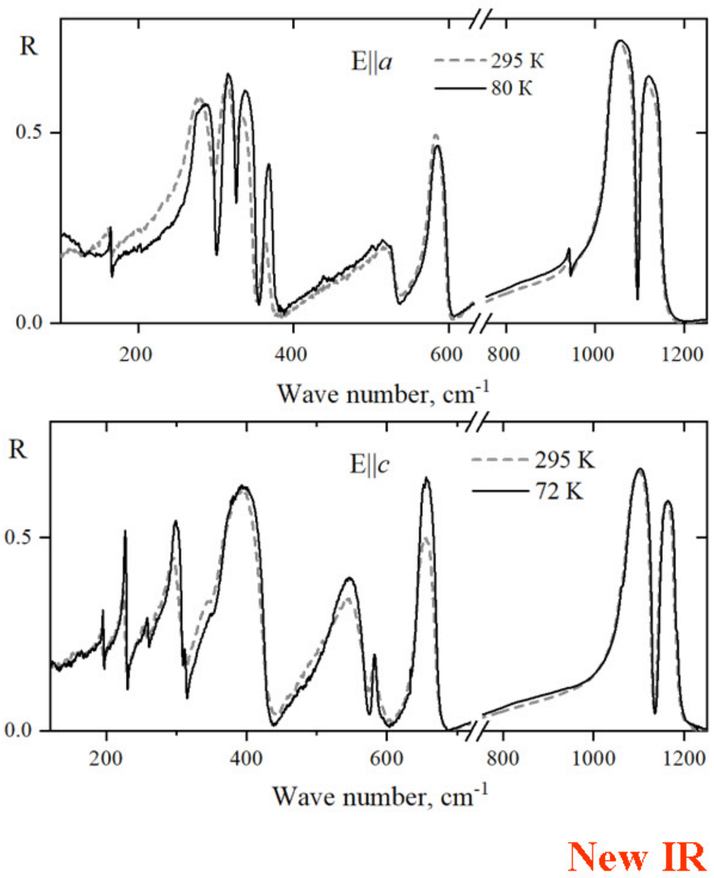

Table 1. Optical parameters of phonons of the B_{1u}, B_{2u} (70 K), and B_{3u} (80 K) symmetry: frequencies of transverse vibrations ν_{TO}, plasma frequencies ω_P, and half-widths γ (all in cm^{-1})

B_{2u}			B_{3u}			B_{1u}		
ν_{TO}	ω_P	γ	ν_{TO}	ω_P	γ	ν_{TO}	ω_P	γ
207	89	4	165	36	1.8	196	36	1
237	305	11.3	203.3	13.8	1.8	226.6	99	2
265	67	4.7	282.3	323	11.6	259	68	4.9
361	153	8.3	311.6	208	5.9	297	245	8.4
448	198	14	330	132	9.2	311	44	2.8
474.3	328	20.5	362.8	86.6	5.1	346.8	100	21.20
548.1	248	11	510.8	281	33	374	398	18.3
955.1	716	27	578.8	234	9.1	528	356	31
			660.3	174.1	6.1	580	63	4.6
			941.6	131	5.9	646	227	5.3
			1032.6	708	14.9	1075	638	17.5
			1101.7	182	8.9	1145	196	9.1

T_N = 21.8 K , magnetic group $Pnm'a$ (Z=4).

(T_N = 20.8 K – commensurate (C) antiferromagnetic phase, T_c = 21.8 K - incommensurate (IC) antiferro-magnetic phase, above 21.8 K - paramagnetic phase).

Linear magnetoelectric (ME) – $P_i = \alpha_{ij} H_j$

ME coefficients:

$|\alpha_{xz}|$ (4.2 K) = 0.5 ps/m and $|\alpha_{zx}|$ (4.2 K) = 1.5 ps/m .

$\Gamma_{vib}=11A_g+7B_{1g}+11B_{2g}+7B_{3g}+10A_u+14B_{1u}+10B_{2u}+14B_{3u}$

$\Gamma_{ak} = B_{1u}+B_{2u}+B_{3u}$

$\Gamma_{int}= 6A_g + 3B_{1g} + 6B_{2g} +3B_{3g} + 3A_u +6B_{1u} +3B_{2u}+6B_{3u}$,

$\Gamma_{tr} = 4A_g + 2B_{1g} + 4B_{2g} + 2B_{3g} + 5A_u + 6B_{1u} + 4B_{2u} +6B_{3u}$,

$\Gamma_{lib}= A_g+2B_{1g}+B_{2g}+2B_{3g}+2A_u+B_{1u}+2B_{2u}+B_{3u}$

$13B_{1u}$ (E||c) + $9B_{2u}$ (E||b) +$13B_{3u}$ (E||a) modes are active in IR spectra.

New IR data

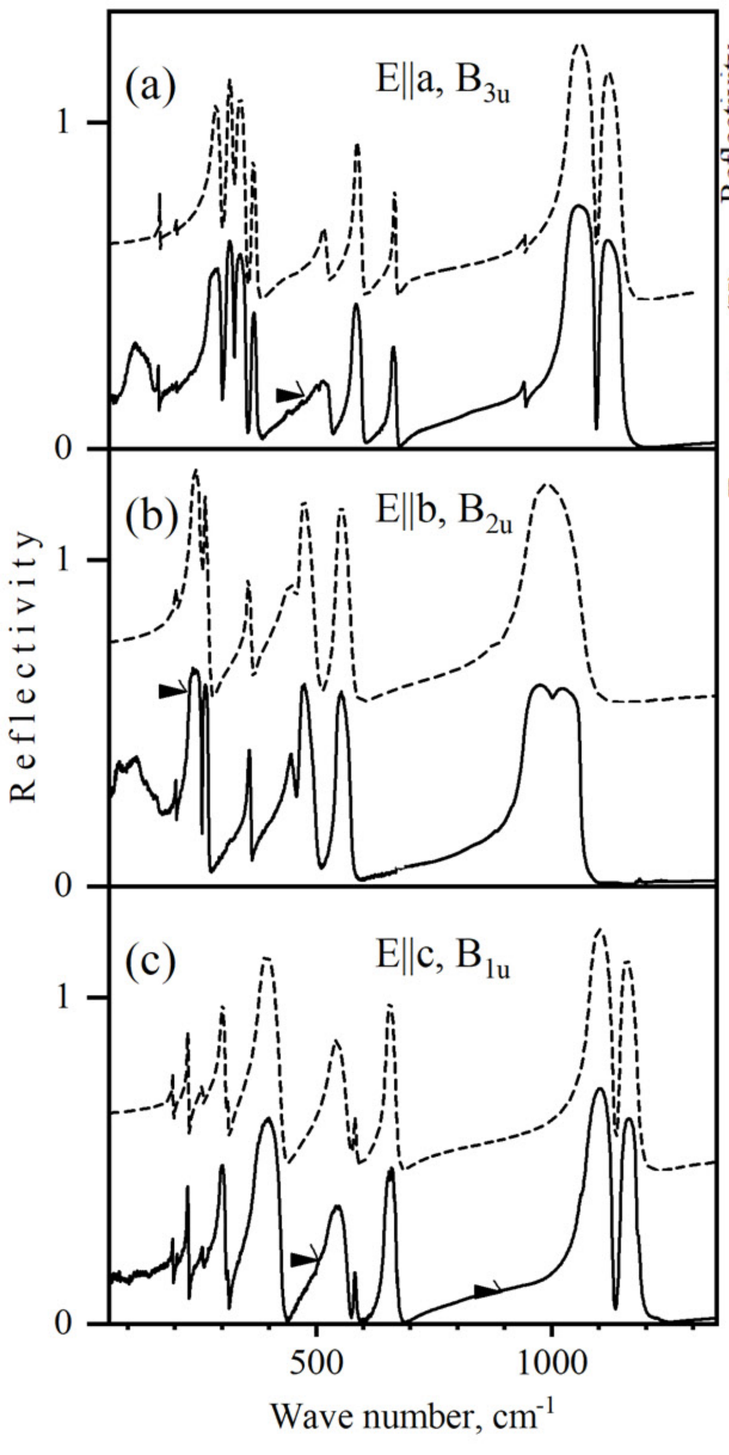

Fig. 4. IR-reflectivity experimental 30 K (solid lines) and modeled (dashed lines) spectra for different polarizations: (a) E||a, B_{3u}- modes, (b) E||b, B_{2u}-modes, (c) E||c, B_{1u}-modes.

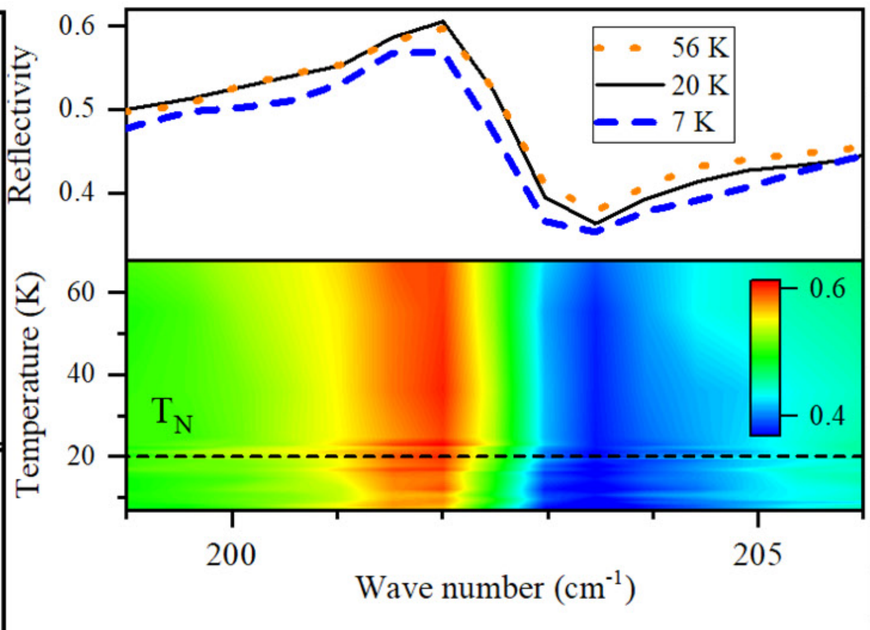

Fig. 5. IR spectra of $LiNiPO_4$ single crystal taken in the E||b polarization at different temperatures and color map IR spectral intensity.

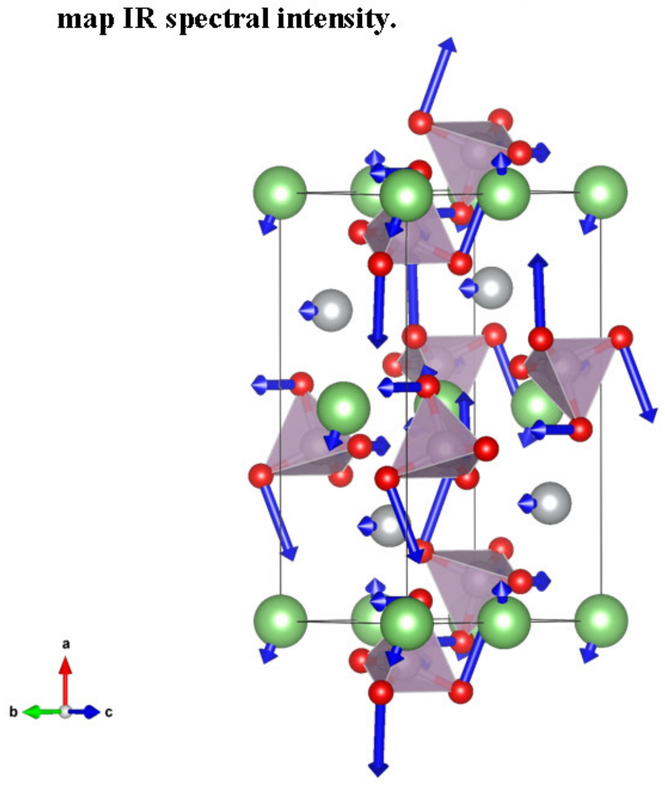

Fig. 6. Vibrational eigenvectors of the calculated 194 cm^{-1} (B_{2u}) phonon mode shown in the unit cell of $LiNiPO_4$.

Table 2. List of the experimentally observed and calculated frequencies of the B_{1u}, B_{2u}, and B_{3u} phonon modes.

B_{1u}		B_{2u}		B_{3u}	
Exp. (cm^{-1})	Calc. (cm^{-1})	Exp. (cm^{-1})	Calc. (cm^{-1})	Exp. (cm^{-1})	Calc. (cm^{-1})
196	177	-	167	165.2	152
227	188	202.3	194	203.5	169
259	237	236	234	-	242
300	258	260	293	285	273
311	312	356.6	303	313	297
382	379	444	427	330.6	365
	456	466	510	363	463
534	542	543	554	514	531
581	596	951	841	580.6	576
650	675			662.5	647
-	937			942	937
1083	1063			1035	977
1145	1175			1102	1111

Conclusions

The analysis of the taken spectra, for the first time, has revealed a number of the phonons indicating the strong coupling between the magnetic and lattice excitations. The B_{2u} mode demonstrates the anomalous behavior during the transition to the magnetically ordered state (see Fig. 5). The displacement vectors for the indicated mode were determined by performing the calculation using the GULP package (Fig. 6) [3]. This mode is assigned to the complex normal vibration including the librations of the PO_4 tetrahedra, out-of-plane vibrations of the Li atoms, and the in-plane vibrations of the magnetic Ni atoms along b-axis, indicating its coupling to the magnetic subsystem. The temperature behavior of this mode reflects the significant spin-phonon coupling at T_N. The detected phonon shift at T_N can be explained by the striction phenomena.

References

[1] T.B.S. Jensen, N.B. Christensen, M. Kenzelman, H.M. Renner et al., Phys. Rev. B79, 092412 (2009).

[2] S.A. Klimin, M.S. Radionov, V.A. Yakovlev, N.N. Novikova, and A.V.Peschanskii, Optics and Spectroscopy 129, 42-46 (2021).

[3] G.D. Gale, GULP: A computer program for the symmetry-adapted simulation of solids, J. Chem. Soc., Faraday Trans. 93, 629-637 (1997).